

Thermo- and pH-Responsive Dendronized Copolymers of Styrene and Maleic Anhydride Pendant with Poly(amidoamine) Dendrons as Side Groups

Min Gao,[†] Xinru Jia,^{†,*} Guichao Kuang,[†] Yan Li,[†] Dehai Liang,^{†,*} and Yen Wei^{‡,*}

[†]Beijing National Laboratory for Molecular Sciences, Key Laboratory of Polymer Chemistry and Physics of the Ministry of Education, College of Chemistry and Molecular Engineering, Peking University, Beijing 100871 China, and [‡]Department of Chemistry, Drexel University, Philadelphia, Pennsylvania 19104

Received January 14, 2009; Revised Manuscript Received April 27, 2009

ABSTRACT: A series of thermo- and pH-dual responsive dendronized polymers **PSADG1–PSADG3** were successfully synthesized by attaching butylamide terminated poly(amidoamine) dendrons (**DG1–DG3**) to the alternating copolymers of styrene (St) and maleic anhydride (MAh). The structures and the molecular weights of the obtained polymers were characterized by ¹H NMR and FTIR. The coverage degrees of **DG1–DG3** dendrons were 83.5%, 64.9%, and 60.5%, respectively, indicating that the numbers of the attaching dendrons decreased in the order of G1 > G2 > G3. The turbidity measurements revealed that all the dendronized polymers exhibited reversible thermo-responsive property in deionized water, and the LCST values increased from **PSADG1** to **PSADG3** due to both the coverage degree and the structure of dendrons. Moreover, these dendronized polymers were sensitive to pH on account of the carboxylic and tertiary amino groups in the architecture. It has been found that, for example, the **PSADG2** did not display thermal sensitivity in acidic environment (pH 2.4), whereas the phase transition occurred in near neutral (pH 6.0) and basic conditions (pH 10.6) with the LCST of 33.1 and 49.0 °C, respectively. It was also found that, at pH 6.0, the polymers formed larger aggregates with $R_{h,app}$ of ca. 0.6 μm at elevated temperatures mainly because of the dehydration and the enhanced hydrophobic interactions. The morphology of the aggregates was monitored by optical microscopy, and uniform spherical aggregates with a diameter of 5–10 μm were observed above the LCST.

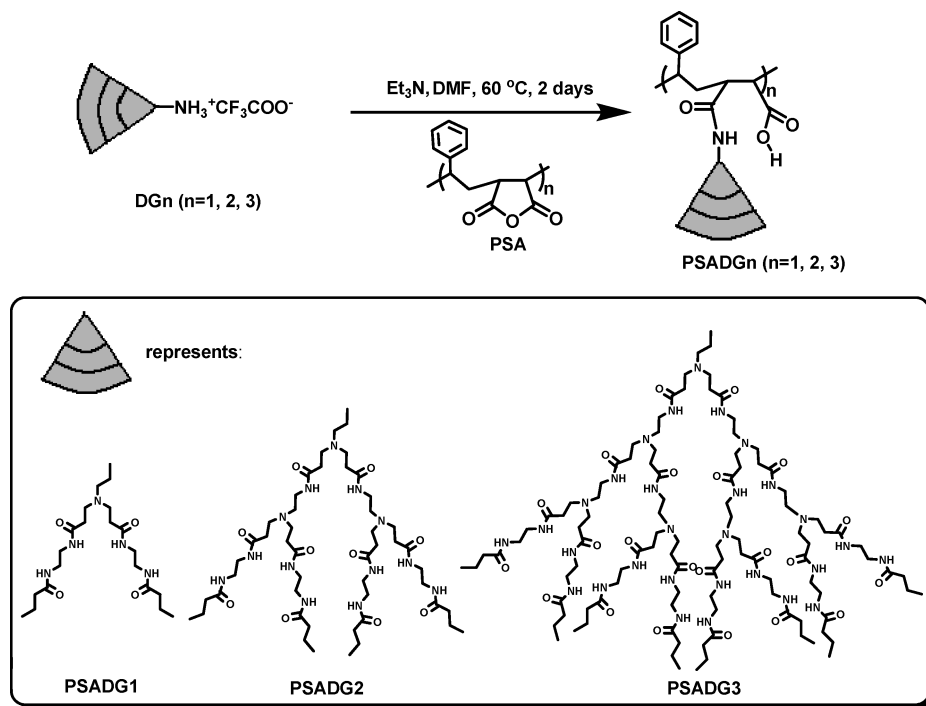
Introduction

Stimuli-responsive polymers, also known as “smart polymers” or “intelligent polymers”, have attracted a great deal of interest in many fields for their functioning in much the same way as biopolymers in living organisms¹ as well as their wide applications in drug delivery, gene carriers, tissue engineering, sensors, catalysis, and chromatography separation.^{2–7} The major characteristic of the stimuli-responsive polymers is their capacity in response to small variations of environmental conditions (pH, temperature, light, ionic factors, etc.) with large and abrupt changes in shape, volume, and phase state or electrical, mechanical, and surface properties. Besides the single-responsive polymers,^{8–11} polymers with dual- or multiresponsive properties, such as thermo- and pH-dual responsive ones,^{12–18} have received much more attention in the past several decades. For example, Stöver and Yin¹³ synthesized the copolymers of maleic anhydride and styrene (or 4-*tert*-butylstyrene) grafted with methoxy poly(ethylene glycol). They reported that the lower critical solution temperatures (LCSTs) of these amphiphilic copolymers exhibited high sensitivity to pH and salinity due to the cooperative effects of hydrophobic and intra/intermolecular hydrogen-bonding interactions. Müller and co-workers¹⁴ reported that the formation of micelles from poly(*N*-isopropylacrylamide)-*block*-poly(acrylic acid) (PNIPAAm-*b*-PAA) was dependent on pH and

temperature as a consequence of hydrogen-bonding interaction between NIPAAm and AA blocks.

Besides the chemical property of the thermo-responsive units, the location and the special distribution of these units also showed great effect on the responsiveness of the polymers. Kono et al.¹⁹ developed a kind of thermo-sensitive polymer with a globular structure by modifying the terminals of poly(amidoamine) (PAMAM) dendrimers with *N*-isopropylamide (NIPAM) groups. These NIPAM-terminated dendrimers underwent a sharp phase transition and showed much lower transition enthalpies resulting from the densely packing of NIPAM groups on the periphery. Chen and co-workers²⁰ synthesized the hyperbranched polyethylenimines ended with isobutyramide (IBAM) groups. They reported that the LCST of the polymers depended highly on the molecular weight owing to the compact spherical topology. From this point of view, as a new class of macromolecules, the dendronized polymers consisting of linear polymers bearing dendrons as side groups are active candidates with considerable importance for tailoring the stimuli-responsive properties because of their unique architecture. Over the last 20 years, various dendronized polymers were synthesized and reported by the pioneers, such as Tomalia,²¹ Schlüter and Zhang,^{22–26} Fréchet,^{27–30} Percec,^{31–33} Xi,^{34–37} and Chen^{38,39} et al. The polymers with such architecture were reported to afford the advantages of self-assembly into nanoscopic objects such as LC phase,⁴⁰ construction of functional materials,⁴¹ development of efficient and stable blue-emitting materials,⁴² participation in single molecule reactions and surface patterning,⁴³ and mimicking the functions of the biological molecules.⁴⁴

*Corresponding author. (X.J.) Telephone: +86 10 62752102. Fax: +86 10 62751708. E-mail: xjia@pku.edu.cn. (D.L.) Telephone: +86 10 62756170. Fax: +86 10 62751708. E-mail: dliang@pku.edu.cn. (Y.W.) Telephone: +1 215 895 2652. Fax: +1 215 895 1265. E-mail: weiyen@drexel.edu.

Scheme 1. Synthesis and Structures of PSADGn ($n = 1, 2, 3$)

However, little attention has been paid to the dendronized polymers with stimuli-responsive properties. The dendronized polymers with thermo- and pH-dual responsive behaviors are still rare. Zhang et al.⁴⁵ synthesized a series of water-soluble block copolymers consisting of thermo-responsive poly(*N*-isopropylacrylamide) (PNIPAAm) and positively charged dendronized polymethacrylate as building blocks. They reported that these copolymers exhibited thermally switchable aggregation behavior with the lower critical aggregation temperatures (LCATs) in the range of 33–43 °C. Recently, they synthesized a series of first (PG1) and second (PG2) generation dendronized polymethacrylate derivatives, using gallic acid as branching point and oligoethylene glycol (OEG) units as the linker. All these polymers exhibited sharp phase transitions in aqueous solution in the range of 33–65 °C with negligible hystereses.^{46,47} For comparison, they also synthesized thermo-responsive dendrimers (G1 and G2) based on 3-fold branched OEG dendrons. They found that the concentration and generation dependence of LCST were lower for the dendronized polymers than for the corresponding dendrimers.⁴⁸

Herein, we report the synthesis of thermo- and pH-dual responsive dendronized polymers **PSADGn** (Scheme 1, $n = 1, 2, 3$) by grafting butylamide terminated poly(amidoamine) dendrons (**DG1–DG3**) to an alternating copolymer of styrene (St) and maleic anhydride (MAh) via a ring-opening reaction. The structures, thermo- and pH-dual responsive properties were studied by ¹H NMR, FTIR, UV–vis, laser light scattering (LLS), and optical microscopy. All the obtained polymers were thermo-responsive and pH sensitive in deionized water. The lower critical solution temperatures (LCSTs), which were dependent on concentration, ionic strength (NaCl), and pH, were determined by the turbidity measurement.

Experimental Section

Materials. Poly(amidoamine) dendrons **DGn** ($n = 1–3$) (Scheme 1) were synthesized according to the method reported previously.⁴⁹ PSt-*alt*-MAh copolymer (**PSA**) was kindly

provided by Professor Zichen Li's group with the number molecular weight of 10800 and the polydispersity of 1.32. *N,N*-Dimethylformamide, triethylamine, and tetrahydrofuran were purchased from Chemical Reagent Beijing Co. and purified according to the standard procedures. Unless stated otherwise, all the reagents and the common solvents were obtained from commercial sources and used as received.

Measurements. ¹H NMR was recorded on 300 MHz (Varian Mercury) and 400 MHz (Bruker) spectrometers operated at room temperature and 50 °C, respectively, with acetone-*d*₆ or DMSO-*d*₆ as the solvents and tetramethylsilane (TMS) as the internal standard. FTIR spectra were obtained on a VECTOR 22 Fourier transform IR spectrometer (Bruker). For UV–vis turbidity measurements, the LCSTs were determined on a Varian CARY 1E UV–vis spectrophotometer, equipped with a BECKMAN 9112AA2E (PolyScience) thermostatic bath. The heating rate was about 0.5 °C/min. The temperature of the phase transition (LCST) was defined as the one corresponding to the initial break points in the resulting transmittance (at $\lambda = 550$ nm) versus temperature curve. A gel permeation chromatograph (GPC) equipped with a Waters 410 refractive-index detector, a Waters 515 HPLC pump, and Ultrastaygel columns (104, 103, and 500 Å) with THF as an eluent at a flow rate of 1.0 mL/min. Monodispersity polystyrene standards were used for calibration. Differential scanning calorimetry (DSC) measurements were carried out on TA Instruments DSC Q100. Polymer samples were sealed in aluminum pans. An empty aluminum pan was used as the reference. A scanning rate of 10.0 °C/min was used for both heating and cooling processes between 20 and 160 °C. The glass transition temperature (T_g) was obtained from the second heating run and corresponded to the midpoint of discontinuity in the heat flow. The dynamic light scattering (DLS) experiments of **PSADG2** at 0.25 mg mL^{−1} in aqueous solution at different pHs were performed on a Brookhaven goniometer (BI-200SM) equipped with a BI-TurboCorr digital correlator and a thermostatic bath with temperature accuracy of 0.01 °C. A vertically polarized solid-state laser operating at 532 nm was used as the light source (100 mW, CNI Changchun GXC-III, China). The stock solutions were

filtered through a Millipore 0.45 μm PVDF filter into a dust-free vial. During heating, the autocorrelation functions were collected when the excess scattered intensity at each temperature became stable. The time correlation functions were analyzed with a Laplace inversion program CONTIN. Optical microscopy images of **PSADG2** solution were recorded using a Leica DLMP microscope. The polymer solution was placed in a glass liquid sample cell and covered with a glass slide. Then the sample was heated from room temperature to 50 $^{\circ}\text{C}$ with the heating rate of 1 $^{\circ}\text{C}/\text{min}$. The micrographs were recorded by a Digital sight camera at a specific temperature in the process.

Synthesis of PSA Copolymers. The synthetic procedure was as follows: 4.9 g (0.05 mol) of maleic anhydride, 5.2 g (0.05 mol) of styrene, and 0.0154 g (0.1 mmol) of AIBN were dissolved in 40 mL of acetone in a Schlenk tube. Then 0.146 g (0.5 mmol) of 2-phenylpropan-2-yl phenyldithioacetate (PPDA), as chain transfer agent, was added. After the solution was thoroughly deoxygenated by three freeze–pump–thaw cycles, the tube was sealed and heated to 60 $^{\circ}\text{C}$ for 24 h. After being cooled to room temperature, the product was purified by precipitation twice from acetone/petroleum ether and dried under vacuum for 24 h. The structure and molecular weight of the copolymer were determined by ^1H NMR, FTIR, and GPC. ^1H NMR (300 MHz, acetone- d_6 , TMS, $T = 298\text{ K}$): 7.60–6.00 (br, Ph H), 3.70–3.00 (br, CH–CH (MAh unit)), 2.85 (br, H_2O), 2.80–2.10 (br, CH_2 –CH (St unit)). ^1H NMR (DMSO- d_6): 7.60–6.00 (br, Ph H), 3.33 (s, H_2O), 3.60–2.80 (br, CH–CH (MAh unit)), 2.80–1.50 (br, CH_3 -DMSO and CH_2 –CH (St unit)). IR (KBr, cm^{-1}): 3033, 2929, 1858, 1778, 1551, 1492, 1451, 1326, 1224, 1085, 954, 917, 759, 700. GPC (THF as eluent): $M_n = 10800$ (DP = 53); PDI = 1.32.

Synthesis of PSADG n ($n = 1, 2, 3$). All the reactions were carried out with DMF as the solvent in a degassed and sealed tube. A representative procedure was as follows: 0.12 g (0.22 mmol, 20% excess) **DG1** and 44.7 mg (0.44 mmol) triethylamine (TEA) were dissolved in DMF. Then the solution was added to a DMF solution of 37.3 mg (0.18 mmol) **PSA** inside a Schlenk tube. After the solution was thoroughly deoxygenated by three freeze–pump–thaw cycles, the tube was sealed and heated to 60 $^{\circ}\text{C}$ for 48 h. After being cooled to room temperature, the obtained DMF solution was slowly dropped into about 40 mL of THF, the precipitate was collected and purified by reprecipitation from methanol/THF. The obtained white precipitate was recovered by filtration and characterized by the combined techniques of ^1H NMR and FTIR.

PSADG1. This was obtained as a white solid. Yield: 77% (90 mg). ^1H NMR (400 MHz, DMSO- d_6 , TMS, $T = 348\text{ K}$): 7.76–7.66 (br, CONH), 7.40–6.00 (br, Ph H), 3.20 (br, $\text{CONHCH}_2\text{CH}_2\text{N}$), 3.10 (br, $\text{NHCH}_2\text{CH}_2\text{NH}$), 2.63 (br, $\text{CH}_2\text{NCH}_2\text{CH}_2$), 2.15 (br, $\text{CH}_2\text{CH}_2\text{CO}$), 2.04 (t, $\text{CH}_2\text{CH}_2\text{CH}_3$), 1.54–1.49 (m, $\text{CH}_2\text{CH}_2\text{CH}_3$), 0.87–0.83 (t, $\text{CH}_2\text{CH}_2\text{CH}_3$) (note: CH_2 and CH in the main chain were at 2.0–4.0 ppm and they were shielded by the signals of protons in the dendrons on the side chain). IR (KBr, cm^{-1}): 3414, 3088, 2960, 2874, 1779, 1714, 1649, 1549, 1444, 1391, 1241, 1130, 1032, 758, 702.

PSADG2. This was obtained as a light yellow solid (moisture-sensitive). Yield: 79% (145.3 mg). ^1H NMR (400 MHz, DMSO- d_6 , TMS, $T = 348\text{ K}$): 7.90–7.70 (br, CONH), 7.50–6.00 (br, Ph H), 3.20 (br, $\text{NHCH}_2\text{CH}_2\text{N}$), 3.12 (br, $\text{NHCH}_2\text{CH}_2\text{NH}$), 2.82 (br, $\text{NCH}_2\text{CH}_2\text{CO}$), 2.62 (br, $\text{NHCH}_2\text{CH}_2\text{N}$), 2.29–2.15 (br, $\text{CH}_2\text{CH}_2\text{CO}$), 2.06–2.03 (t, $\text{CH}_2\text{CH}_2\text{CH}_3$), 1.56–1.49 (m, $\text{CH}_2\text{CH}_2\text{CH}_3$), 0.87–0.83 (t, $\text{CH}_2\text{CH}_2\text{CH}_3$) (note: CH_2 and CH in the main chain were at 2.0–4.0 ppm and they were shielded by the signals of protons in the dendrons on the side chain). IR (KBr, cm^{-1}): 3446, 3081, 2963, 2934, 2874, 1768, 1695, 1645, 1557, 1456, 1437, 1383, 1242, 1202, 1128, 1093, 1034, 703.

PSADG3. This was obtained as a yellow solid (moisture-sensitive). Yield: 66% (106.7 mg). ^1H NMR (400 MHz, DMSO- d_6 , TMS, $T = 348\text{ K}$): 7.85–7.68 (br, CONH), 7.50–6.00

(br, Ph H), 3.26 (br, $\text{NHCH}_2\text{CH}_2\text{N}$), 3.11 (br, $\text{NHCH}_2\text{CH}_2\text{NH}$), 2.77 (br, $\text{NCH}_2\text{CH}_2\text{CO}$), 2.56 (br, $\text{NHCH}_2\text{CH}_2\text{N}$), 2.26 (br, $\text{CH}_2\text{CH}_2\text{CO}$), 2.06–2.02 (t, $\text{CH}_2\text{CH}_2\text{CH}_3$), 1.54–1.48 (m, $\text{CH}_2\text{CH}_2\text{CH}_3$), 0.87–0.84 (t, $\text{CH}_2\text{CH}_2\text{CH}_3$) (note: CH_2 and CH in the main chain were at 2.0–4.0 ppm and they were shielded by the signals of protons in the dendrons on the side chain). IR (KBr, cm^{-1}): 3445, 3084, 2964, 2938, 2875, 1866, 1768, 1696, 1646, 1557, 1459, 1438, 1382, 1282, 1246, 1203, 1131, 1064, 1036, 705.

Results and Discussion

Synthesis of Dendronized Polymers. **PSA** copolymer was synthesized by reversible addition–fragmentation transfer (RAFT) polymerization with the number average molecular weight of 10800 and the polydispersity of 1.32 characterized by GPC (Figure S1). **DG n** ($n = 1–3$) were obtained by the coupling reaction of amino-terminated poly(amidoamine) dendrons with excess butyric acid in the presence of 1,3-dicyclohexylcarbodiimide (DCC) and further removing the Boc group with trifluoroacetic acid.⁴⁹ As shown in Scheme 1, the butylamide terminated poly(amidoamine) dendrons **DG n** were then attached to the backbone of **PSA** polymer by a ring-opening reaction of exposed NH_2 with maleic anhydride groups.

The structures and molecular weights of the resulting dendronized polymers were confirmed by ^1H NMR and FTIR. Figure 1 shows the ^1H NMR spectra of **PSA** (1a) and **PSADG1** (1b), respectively. Due to the shielding effect of the dendrons, the protons of CH_2 and CH at 2.00–4.00 ppm in the main chain of **PSA** were not clearly visible in the ^1H NMR spectrum of **PSADG1** (Figure 1b). However, the signals of phenyl protons related to styrene units appeared as a broad peak at 6.00–7.40 ppm. From the integral ratio of the phenyl protons of styrene units and the methyl protons (0.83–0.87 ppm) of the butylamide on the periphery of dendrons, the coverage degrees of **DG1–DG3** dendrons were calculated to be 83.5%, 64.9%, and 60.5%, respectively (Table 1 and Figure S2). Accordingly, the molecular weights of the dendronized polymers were 30000, 46000, and 82000 for **PSADG1**, **PSADG2**, and **PSADG3**, respectively, which were much higher than that of **PSA**. Obviously, the average attaching number of dendrons appeared to decrease in the order of **PSADG1** > **PSADG2** > **PSADG3**, indicating that the first generation dendron reacted with maleic anhydride more readily than the second and third generations. A similar phenomenon was also observed by Schlüter et al.^{50,51} This could be well understood from the architectural effect. The higher generation dendrons with more branches hindered the reaction due to the steric effect.

A FTIR spectrometer was used to further prove the structures of the resulting dendronized polymers. Two changes were observed when comparing the spectra of **PSADG1** and **PSADG2** with that of **PSA** (Figure 2): (1) The stretching vibration of O–H of the carboxylic acid groups and the stretching vibration of N–H of the amide groups were merged as a broad peak at 3414 cm^{-1} ; (2) The peaks at 1858 and 1778 cm^{-1} , which were related to the stretching vibration of C=O of maleic anhydride units, decreased significantly, while the peaks at 1649 and 1549 cm^{-1} corresponding to amide I ($\nu_{\text{C=O}}$) and amide II ($\delta_{\text{N–H}}$) appeared and well-separated. In addition, a shoulder peak of amide I at 1714 cm^{-1} was observed and attributed to the stretching vibration of C=O of carboxylic acid groups. These results indicated that the dendrons were successfully attached to the backbone of **PSA**. However, for **PSADG3**,

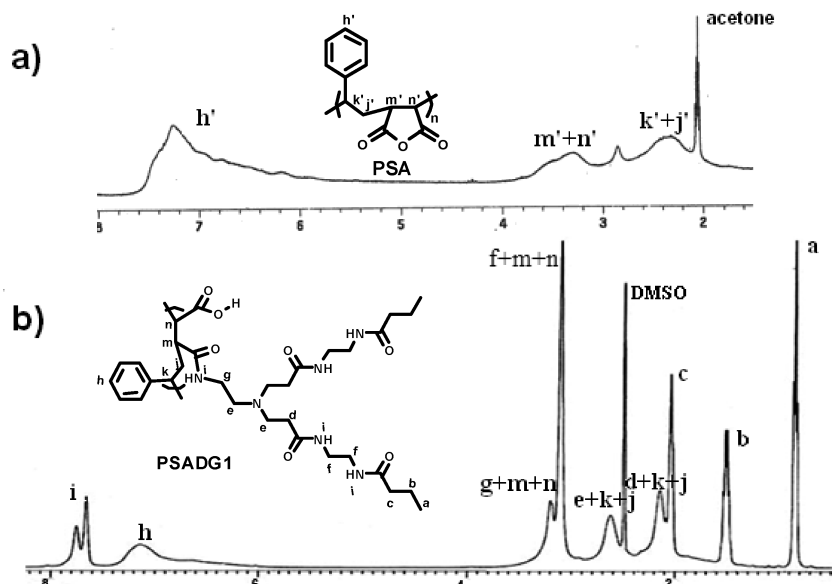


Figure 1. ^1H NMR spectra of (a) PSA (acetone- d_6 , 298 K) and (b) PSADG1 (DMSO- d_6 , 348 K).

Table 1. Properties of the Dendronized Polymers PSADG n ($n = 1, 2, 3$)

polymers	degree of coverage ^a (g) (%)	yield (%)	molecular weight	T_g (°C) ^f	LCST in water ^d (°C)	LCST in 0.1 M NaCl ^d (°C)	discrepancy ^e (°C)
PSA			10800 (1.32) ^c	180			
PSADG1	83.5	77	30000 ^b	60.1	5.6	5.4	0.2
PSADG2	64.9	79	46000 ^b	49.5	32.6	29.7	2.9
PSADG3	60.5	66	82000 ^b	36.8	~65.7	27.6	~38.1

^a Calculated from ^1H NMR determined at 50 °C. ^b Calculated from ^1H NMR (50 °C) through the formula $M_w = 10800 + 53 \times (M_{\text{DG}n} - 114) \times g$. $M_{\text{DG}n}$ represents molecular weight of DG n ; 114 represents the molecular weight of CF_3COOH ; g represents degree of coverage; 10800 and 53 represent the molecular weight and degree of polymerization of PSA, respectively; ^c Determined by GPC with THF as the eluent and the PDI value is in the parentheses; ^d Determined by the turbidity measurements; ^e The difference between LCST values in water and 0.1 M NaCl solution; ^f The glass transition temperature (T_g) was determined by DSC analysis under nitrogen.

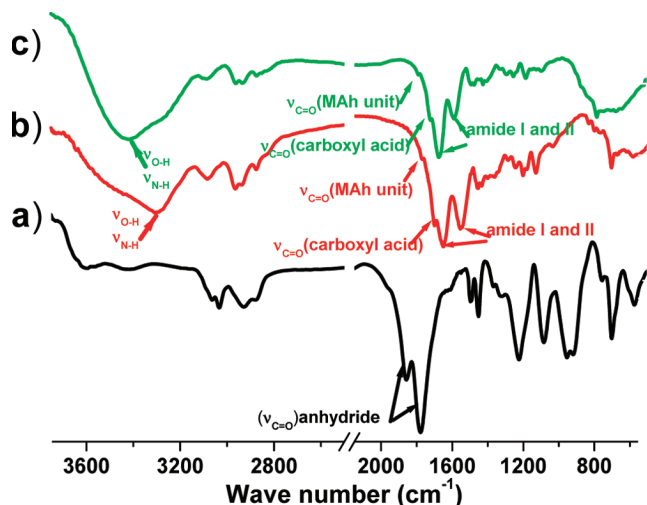


Figure 2. FTIR spectra of (a) PSA, (b) PSADG1, and (c) PSADG2.

the peaks corresponding to the $\nu_{\text{C=O}}$ of the unreacted maleic anhydride units were not obviously visible due to the strong absorption of amide I and II (Figure S3).

Differential scanning calorimetric (DSC) measurement was performed to study the thermo-properties of the resulting dendritic polymers. As shown in Table 1, during the second heating run, the polymers showed glass transition temperature (T_g) at 60.1, 49.5, and 36.8 °C for PSADG1, PSADG2, and PSADG3, respectively. The glass transitions of these dendronized polymers were also observed during the

first cooling run at a cooling rate of 10.0 °C/min (Figure S4b, see the Supporting Information). Compared with that of PSA copolymer (T_g 180 °C), the glass transition temperatures of the dendronized polymers significantly decreased due to the pendant of dendritic units. This result was in accordance with that reported by Khan et al.⁵² They found that the T_g of the ethyl cellulose derivatives functionalized with amidoamine dendrons underwent a significant decrease as a result of the substitution by dendritic appendages. Moreover, the T_g of PSADG n decreased with increasing the generation of dendrons. In our case, the T_g of PSADG n should be dependent on both the generation of attached dendrons and the remained MAh units. It was likely that the generation of dendrons dominated the T_g although the coverage degrees were lower for higher generations. Such results might be mainly due to the dendritic architecture. The higher generation dendrons, such as G2 and G3, attached along the polymer main chain would occupy more room and wrap the polymer chain inside. This might weaken the stiffness of the unreacted maleic anhydride units and endow the resulting polymers with softer nature from the structure of dendrons, leading to a decrease in T_g .

Thermo-Responsive Behavior of PSADG1–PSADG3. UV–vis spectrophotometer was used to measure the transmittance of the solution ($\lambda = 550$ nm) as a function of temperature in order to determine the LCSTs of PSADG1–PSADG3. Figure 3a shows the transmittance change of PSADG1, PSADG2, and PSADG3 at 1.0 mg mL⁻¹ in aqueous solutions during the heating and cooling processes. All the dendronized polymers exhibited phase transitions in

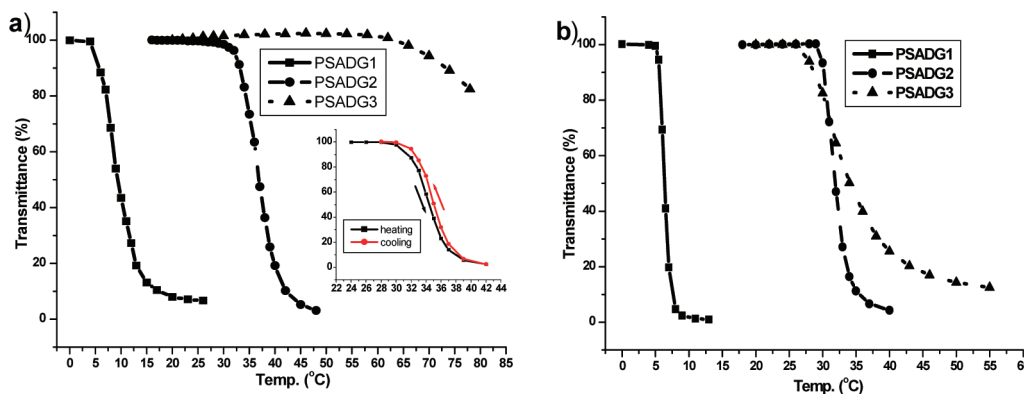


Figure 3. Temperature dependence of the transmittance of (a) 1 mg mL⁻¹ aqueous solution and (b) 1 mg mL⁻¹ 0.1 M NaCl solution of **PSADG1** (■, solid line), **PSADG2** (●, dashed line) and **PSADG3** (▲, dotted line). Inset of part a: the plots of transmittance vs temperature for 1 mg mL⁻¹ aqueous solution of **PSADG2** during one heating and cooling cycle.

deionized water, and their thermo-responsive behavior was reversible. For **PSADG1**, the solution turned turbid at 5.6 °C. However, the solutions of **PSADG2** and **PSADG3** became cloudy at higher temperatures of 32.6 and 65.7 °C, respectively. Notably, **PSADG1** and **PSADG2** showed relatively sharp transitions during both the heating and cooling processes. As shown in the inset of Figure 3a, the span of hysteresis for **PSADG2** was 0.5 °C. However, a relative broad transition zone appeared for **PSADG3**. These results demonstrated that the generation of the pendant dendrons impacted the phase transition greatly, and the low generation dendrons facilitated the collapse of the polymers. It is well-known that the ratio of the hydrophobic and hydrophilic units in a polymer chain alters LCST, and a desired LCST could be achieved by incorporating a suitable portion of hydrophobic or hydrophilic constituent.^{53,54} Generally, hydrophilic segments would result in higher LCST,⁵⁵ and hydrophobic units had the tendency to decrease LCST.⁵⁶ Structurally, the obtained polymers pendant with dendrons of generations 1–3 possess different hydrophilic and hydrophobic compositions. Although the coverage degrees of dendrons decreased with increasing generation, the numbers of amide groups per dendron molecule increased significantly with the generation. For example, **DG1** dendron contains 4 amide groups, while **DG2** and **DG3** dendrons have 10 and 22 amide groups, respectively. Therefore, the high generation dendronized polymers possessed more amide moieties (G3 (737) > G2 (378) > G1 (221)) that could strongly interact with adjacent water molecules through hydrogen bonds, which would enhance the hydrophilicity of the polymers and thus resulted in a higher LCST and a less sensitive phase transition.

To observe the effect of ionic strength on the thermo-responsive behavior, sodium chloride was introduced to the aqueous solutions. As shown in Figure 3b, the LCSTs of **PSADG1**, **PSADG2**, and **PSADG3** in 0.1 M NaCl aqueous solution decreased to 5.4, 29.7, and 27.6 °C, respectively. The drop-off in LCST was only 0.2 °C for **PSADG1**, but about 38.1 °C for **PSADG3**, indicating the strong influence of ionic strength on the thermo-responsive behavior of the dendronized polymers pendant with high generation dendrons (Table 1). The salting-out effect accompanied by LCST decrease is often observed in the thermo-responsive systems mainly because the anions can polarize adjacent water molecules involved in hydrogen-bonding interaction with the amide groups. Moreover, the hydrophobic hydration of the macromolecules is also interfered by salt species through increasing the surface tension.⁵⁷ In our case, the steep decrease of the phase transition temperature of

PSADG3 in NaCl solution might also result from its structure. Besides having more amide groups (G3 (737) > G2 (378) > G1 (221)), **PSADG3** contained more carboxylic groups (G3 (74) > G2 (72) > G1 (62)) in the backbone derived from both hydrolysis and ring-opening reaction, although its coverage degree was only 60.5%. In the presence of NaCl, the hydrogen bonds among the carboxylic groups, amide groups and water molecules were weakened because the adjacent water molecules were polarized. Therefore, the **PSADG3** polymer displayed higher hydrophobicity, resulting in a further decrease in LCST. Moreover, the addition of NaCl shielded the repulsion between the charged carboxylic groups, which also led to a lower LCST.

The concentration dependence of the LCSTs of these dendronized polymers was also studied. Figure 4a shows the transmittance of **PSADG2** as a function of temperature at different concentrations in 0.1 M NaCl solutions. The LCST increased from 29.7 to 34.9 °C as the concentration decreased from 1.0 to 0.1 mg mL⁻¹ (Figure 4b). In addition, the transition zone became broader upon dilution. This result was consistent with that reported by Liu et al., who found that the LCST values increased and the transition temperature region became broader upon lowering the concentrations of *linear*-PNIPAM-*N*₃ and *cyclic*-PNIPAM.⁵⁸

pH-Responsiveness of the Dendronized Polymers. The resulting dendronized polymers can be considered as zwitterionic copolymers for the coexistence of the carboxylic acid groups in the main chain and the tertiary amino groups in the pendant dendrons. Therefore, **PSADG1**, **PSADG2**, and **PSADG3** displayed different LCSTs at different pHs. Take **PSADG2** as a representative, Figure 5 shows the temperature dependence of the transmittance at pH 2.4, 6.0, and 10.6, respectively. It was found that the solution of **PSADG2** (0.25 mg mL⁻¹) was transparent at pH 2.4 over the experimental temperature range. However, the phase transition occurred at pH 6.0 and 10.6 with the LCSTs of 33.1 and 49.0 °C under the same conditions. As was reported, the ionizable groups could alter the balance of the hydrophilicity and hydrophobicity of the polymers resulting in the change of LCST.^{59,60} For the pendant poly(amidoamine) dendrons, all the tertiary amino groups in the branches would be protonated at pH 2.4,⁶¹ which enhanced the hydrophilicity of the polymers. Moreover, the hydrophobic interaction of the peripheral butylamide groups, as well as that of the carboxylic acid groups (not charged under this condition), was weakened due to the electrostatic repulsion between positively charged tertiary amino groups, which also prevented the aggregation of **PSADG2** at elevated temperatures. This result was similar with that reported by Kono et al., who

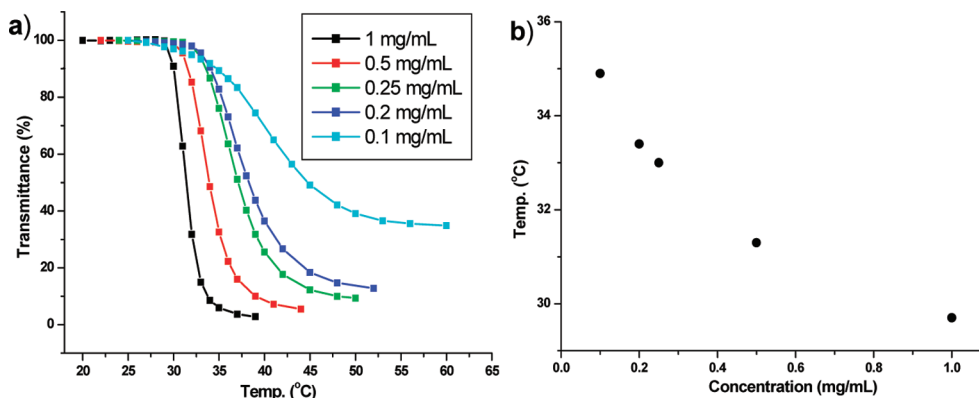


Figure 4. (a) Temperature dependence of the transmittance of **PSADG2** at different concentrations in 0.1 M NaCl solutions; (b) LCSTs of **PSADG2** vs concentration.

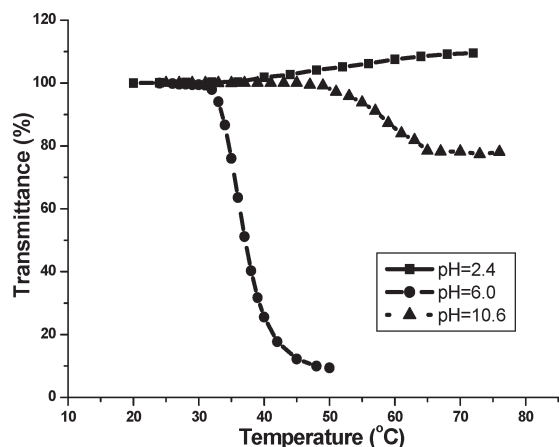


Figure 5. Temperature dependence of the transmittance of 0.25 mg mL⁻¹ **PSADG2** at pH 2.4 (HCl solution, ■, solid line); pH 6.0 (0.1 M NaCl, ●, dashed line); pH 10.6 (NaOH solution, ▲, dotted line).

found that the LCST of peripheral isobutyramide (IBAM) modified PAMAM dendrimers significantly increased at lower pH.⁶² At pH 6.0, the tertiary amino groups of the dendrons were fully deprotonated and a fraction of carboxylic acid groups were ionized,¹³ leading to the polymer backbone slightly charged. In such a situation, the polymer showed a sharp phase transition at 33.1 °C because of the enhanced hydrophobicity of **PSADG2** resulting from the loss of the charges of the tertiary amino groups. In the case of pH 10.6, the carboxylic acid groups were completely ionized,¹³ which would increase the hydrophilicity of the polymer in comparison with that at pH 6.0 resulting in that the phase transition temperature varied from 33.1 to 49.0 °C. Moreover, the remaining transmittance at elevated temperature for the aqueous solution of **PSADG2** with a pH of 10.6 was around 80%, suggesting the aggregates were either not so big or not compact, and thus not capable of scattering light efficiently.⁶³

Laser Light Scattering Studies. Laser light scattering was used to provide a better understanding of the thermally induced phase transition. The change in the size distribution of **PSADG2** (0.25 mg mL⁻¹) was measured by DLS in 0.1 M NaCl solution at variable temperature. As shown in Figure 6a, a bimodal distribution was displayed at 25 °C (below LCST). The fast mode, with $R_{h,app}$ of ca. 4 nm, was attributed to the separated polymer chains. The slow mode, having a negligible amount in number, was probably a kind of association formed by unclarified reasons. Similar association behavior was also observed on PEO-*b*-poly(*N*-isopropylacrylamide) at temperatures far below the transition

point of poly(*N*-isopropylacrylamide).^{64–66} As the temperature increased gradually to 31 °C (around LCST), the ratio of the fast mode decreased, but that of slow mode increased. With temperature further increasing to 36 °C (above LCST), the fast mode disappeared, and the slow mode shifted to the large size direction, indicating the occurrence of strong aggregation. Figure 6b shows the temperature dependence of $R_{h,app}$ of **PSADG2** in 0.1 M NaCl aqueous solution. The $R_{h,app}$ corresponding to the fast mode remained almost the same in the temperature range of 25–36 °C, and it disappeared completely above 36 °C. In contrast, the size of the aggregates corresponding to the slow mode decreased slightly in the temperature range of 25–30 °C, the $R_{h,app}$ of which increased dramatically between 30 and 32 °C. With further increasing temperature to 36 °C, the increase in the size of the aggregates slowed down. At 50 °C, the solution turned to a white opaque suspension, as shown in Figure 6d. No valid light scattering data was obtained. These results demonstrated that the polymers collapsed above LCST because of dehydration of the butylamide units on the periphery of dendrons, and subsequently assembled to aggregates driven by enhanced hydrophobic interactions. With further increasing temperature, the amide-containing hydrophilic dendritic branches located outside became even more adhesive, leading to the conglutination of these aggregates. As a result, strong excess scattered intensity was generated (Figure 6c). The intermolecular hydrogen-bonding interactions and the entanglement of the branches made the aggregates adhere together easily, which was similar to the description in our previous papers.^{67,68}

The effect of pH on the thermo-responsive behavior of **PSADG2** was also investigated by DLS. Figure 6c and Figure S5 show the temperature dependence of the excess scattered intensity of **PSADG2** solutions at pH of 2.4, 6.0, and 10.6, respectively. The excess scattered intensity increased with temperature at pH 6.0 and 10.6, exhibiting a transition temperature of 30.5 and 39.5 °C, respectively. While it remained constant at pH 2.4, which agreed with the turbidity measurements (Figure 5). Accordingly, the size distributions of **PSADG2** at temperatures below and above the transition temperature were measured at different pHs (Figure 7). Three features should be pointed out: (1) At pH 2.4, no obvious change in size distribution was found between 27 and 50 °C, suggesting that the dendronized polymer did not possess thermo-responsive property owing to the enhancement of hydrophilicity of **PSADG2** and the electrostatic interactions between charged tertiary amino groups. (2) At pH 10.6, a bimodal size distribution was observed at 25 °C, while at 46 °C, the fast mode disappeared completely

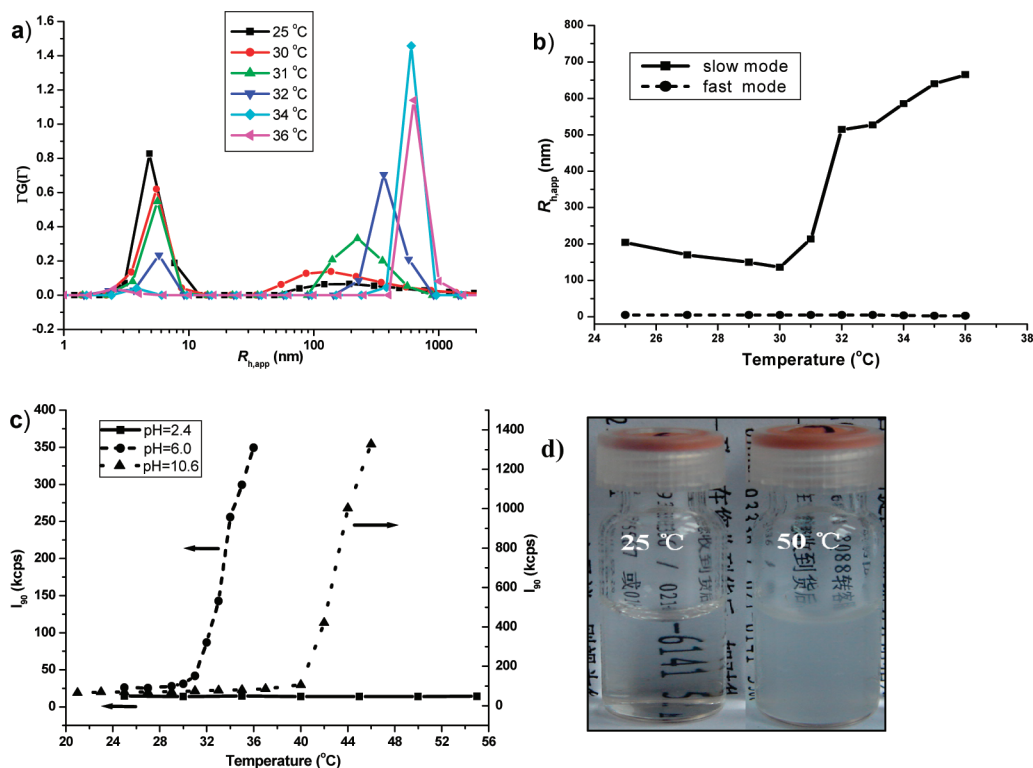


Figure 6. (a) Representative size distributions of PSADG2 (0.25 mg mL^{-1} in 0.1 M NaCl solution, $\text{pH} = 6.0$) determined at 90° at different temperatures. (b) $R_{h,app}$ determined at 90° vs temperature: slow mode (■, solid line); fast mode (●, dashed line). (c) Temperature dependence of the excess scattered intensity of 0.25 mg mL^{-1} PSADG2 at 90° at $\text{pH} 2.4$ (HCl solution, ■, solid line), $\text{pH} 6.0$ (0.1 M NaCl , ●, dashed line), and $\text{pH} 10.6$ (NaOH solution, ▲, dotted line). (d) Photograph of 0.1 M NaCl solution of PSADG2 (0.25 mg mL^{-1}) below and above LCST.

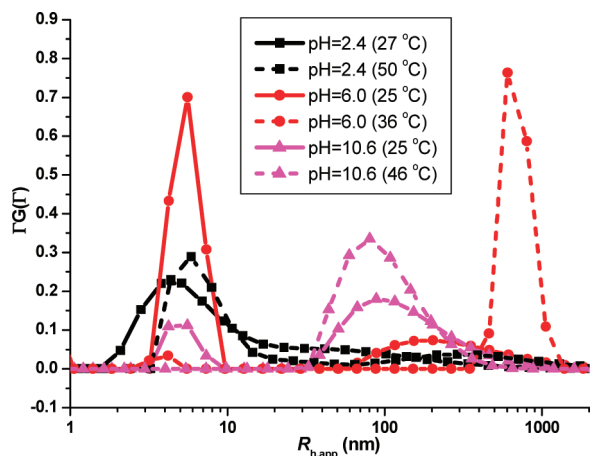


Figure 7. Size distribution curves of 0.25 mg mL^{-1} PSADG2 solutions at temperatures below (solid line) and above (dashed line) the phase transition temperature at $\text{pH} 2.4$ (HCl solution, ■, black curve), $\text{pH} 6.0$ (0.1 M NaCl , ●, red curve), and $\text{pH} 10.6$ (NaOH solution, ▲, pink curve).

and the aggregates with similar $R_{h,app}$ (in the range of 30–500 nm) remained in the system. As indicated in Figures S6 and S7 (see the Supporting Information), the size of the aggregates decreased around 36°C due to the collapse of the dendronized polymer and the hindrance of further aggregation by the repulsion between the negative charges in the main chain. However, as the temperature further increased to ca. 42°C , the $R_{h,app}$ of the aggregates increased on the contrary (Figure S6). The increase in aggregation was induced by the enhanced hydrophobic interactions and the weakened electrostatic repulsion interactions with temperature further increasing. Until the aggregates became big enough, the solution began to turn turbid (49°C as determined

by the UV–vis turbidity determination). (3) At $\text{pH} 6.0$, however, the bimodal distribution was different from that at $\text{pH} 10.6$ at room temperature. The fast mode predominated and the ratio of the slow mode was relatively low at 25°C , similar to the case at $\text{pH} 2.4$. As the temperature increased to 36°C , along with the disappearance of the fast mode, the aggregates with $R_{h,app}$ ranging from 500–2000 nm appeared. Notably, the size of aggregates at $\text{pH} 6.0$ was larger than that at $\text{pH} 10.6$ (Figure 6b and Figure S6), which should be attributed to the inhibition of the intermolecular aggregation by the electrostatic repulsion of the charged sites in the backbone at $\text{pH} 10.6$. All these features demonstrated that the change in size distribution with increasing temperature at different pHs was in accordance with the turbidity measurements (Figure 5) and the excess scattered intensity changes (Figure 6c).

The optical microscopy (OM) was used to visualize the morphology of aggregates directly. Figure 8 shows the typical images of PSADG2 in 0.1 M NaCl solution. Below LCST (28°C), few aggregates were observed. When the temperature increased to 42°C (above LCST), more uniform spherical aggregates with the diameter of $5\text{--}10 \mu\text{m}$ emerged (Figure 8b and inset), indicating the polymers conglomerated into large aggregates with temperature increasing. Such large size aggregates in the aqueous solution were also reported by Zhang et al.^{46,48} The reason for the formation of so large aggregates has not been well understood yet, but many factors, such as hydration and dehydration of the butylamide groups, surface tension and charges might influence the size and morphology of aggregates simultaneously.

Conclusions

Three dendronized polymers PSADG1–PSADG3 were synthesized through the graft-to route by combination of styrene

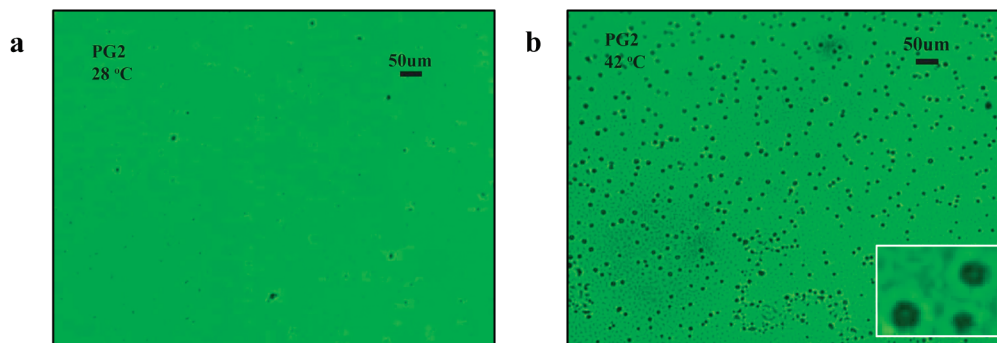


Figure 8. Optical micrographs of **PSADG2** in 0.1 M NaCl solution at (a) 28 °C (below LCST) and (b) 42 °C (above LCST). The concentration of **PSADG2** solution is 0.25 mg mL⁻¹. Image b contains an inset with a 4 times enlarged feature.

and maleic anhydride alternating copolymer and butylamide terminated poly(amidoamine) dendrons with amino group at the focal point. The coverage degrees of the **DG1–DG3** dendrons decreased with the generation increasing and the obtained polymers all exhibited thermo-responsive properties. The LCSTs increased in the order of **PSADG1** < **PSADG2** < **PSADG3** due to the changes of coverage degree and structure of dendrons. It was also observed that the thermo-responsiveness of **PSADGn** was dependent on the concentration and ionic strength. Moreover, these polymers were sensitive to pH for the existence of the carboxylic acid and tertiary amino groups in the architecture. For example, the **PSADG2** did not display thermal sensitivity in acidic environment (pH 2.4), whereas the phase transition occurred in near neutral and basic milieu (pH 6.0 and 10.6) with the LCST of 33.1 and 49.0 °C, respectively. DLS experiments at variable temperatures demonstrated that the polymers aggregated to form larger aggregates with $R_{h,app}$ of several hundred nanometers through dehydration and strengthened hydrophobic interactions as temperature increased. The morphology of **PSADG2** aggregates was monitored by optical microscopy and almost uniform spherical aggregates with the diameter of 5–10 μ m formed above LCST.

In conclusion, we have created a new kind of thermo- and pH-dual responsive dendronized polymer with the concrete arrangement of hydrophilic and hydrophobic units that differs from conventional ones. The LCSTs of the resulting polymers could be tuned by changing generation and coverage degree of the dendrons, by altering the concentration of the polymers, and also by adding salt and changing pH of the solutions. Such materials may become potential candidates spanning a broad temperature range for drug delivery, sensors, and separation materials etc. However, due to the deficiency of the graft-to route, the structures of these dendronized polymers were not defined or well controlled. The synthesis of well-defined and controllable dendronized polymers bearing stimuli-responsive groups is now underway. It can be predicted that stimuli-responsive dendronized polymers will possess more fascinating characteristics and display better performance for various applications.

Acknowledgment. This work was financially supported by the National Natural Science Foundation of China by grants (NSFC 20774003 and 20640420562) to X.J. The authors thank Prof. Zichen Li and Dr. Wenxi Ji for the helpful supply of **PSA** alternating copolymer.

Supporting Information Available: Figures showing the GPC curve of **PSA**, ¹H NMR spectra of **PSADG2** and **PSADG3**, FTIR spectra of **PSADG3**, DSC curves of **PSADGn** during the second heating and first cooling run, temperature dependence of the excess scattered intensity at the scattering angle of 30° at different pHs, temperature dependence of $R_{h,app}$

at pH 10.6, and the representative size distributions of **PSADG2** (pH = 10.6) at different temperatures. This material is available free of charge via the Internet at <http://pubs.acs.org>.

References and Notes

- (1) Gil, E. S.; Hudson, S. M. *Prog. Polym. Sci.* **2004**, *29*, 1173–1222.
- (2) Ganta, S.; Devalapally, H.; Shahiwala, A.; Amiji, M. J. *Controlled Release* **2008**, *126*, 187–204.
- (3) Kumar, A.; Srivastava, A.; Galaev, I. Y.; Mattiasson, B. *Prog. Polym. Sci.* **2007**, *32*, 1205–1237.
- (4) Schmaljohann, D. *Adv. Drug Deliver. Rev.* **2006**, *58*, 1655–1670.
- (5) Alarcón, C. de las, H.; Pennadam, S.; Alexander, C. *Chem. Soc. Rev.* **2005**, *34*, 276–285.
- (6) Jeong, B.; Gutowska, A. *Trends Biotechnol.* **2002**, *20*, 305–311.
- (7) Kikuchi, A.; Okano, T. *Prog. Polym. Sci.* **2002**, *27*, 1165–1193.
- (8) Schild, H. G. *Prog. Polym. Sci.* **1992**, *17*, 163–249.
- (9) Kumar, A.; Srivastava, A.; Galaev, I. Y.; Mattiasson, B. *Prog. Polym. Sci.* **2007**, *32*, 1205–1237.
- (10) Rzaev, Z. M. O.; Dinçer, S.; Pişkin, E. *Prog. Polym. Sci.* **2007**, *32*, 534–595.
- (11) Ganta, S.; Devalapally, H.; Shahiwala, A.; Amiji, M. J. *Controlled Release* **2008**, *126*, 187–204.
- (12) Yuk, S. H.; Cho, S. H.; Lee, S. H. *Macromolecules* **1997**, *30*, 6856–6859.
- (13) Yin, X.; Stöver, H. D. H. *Macromolecules* **2002**, *35*, 10178–10181.
- (14) Schilli, C. M.; Zhang, M.; Rizzardo, E.; Thang, S. H.; Chong, Y. K.; Edwards, K.; Karlsson, G.; Müller, A. H. E. *Macromolecules* **2004**, *37*, 7861–7866.
- (15) González, N.; Elvira, C.; Román, J. S. *Macromolecules* **2005**, *38*, 9298–9303.
- (16) Yin, X.; Hoffman, A. S.; Stayton, P. S. *Biomacromolecules* **2006**, *7*, 1381–1385.
- (17) Wan, S.; Jiang, M.; Zhang, G. *Macromolecules* **2007**, *40*, 5552–5558.
- (18) Wu, D.-C.; Liu, Y.; He, C.-B. *Macromolecules* **2008**, *41*, 18–20.
- (19) Haba, Y.; Kojima, C.; Harada, A.; Kono, K. *Angew. Chem., Int. Ed.* **2007**, *46*, 234–237.
- (20) Liu, H.; Chen, Y.; Shen, Z. *J. Polym. Sci., Part A: Polym. Chem.* **2007**, *45*, 1177–1184.
- (21) Tomalia, D. A.; Kirchoff, P. M. US 06/834993, **1986**.
- (22) Neubert, I.; Schlüter, A. D. *Macromolecules* **1998**, *31*, 9372–9378.
- (23) Zhang, A.; Okrasa, L.; Pakula, T.; Schlüter, A. D. *J. Am. Chem. Soc.* **2004**, *126*, 6658–6666.
- (24) Zhang, A.; Barner, J.; Gössel, I.; Rabe, J. P.; Schlüter, A. D. *Angew. Chem., Int. Ed.* **2004**, *43*, 5185–5188.
- (25) Kasëmi, E.; Zhuang, W.; Rabe, J. P.; Fischer, K.; Schmidt, M.; Colussi, M.; Keul, H.; Yi, D.; Cölfen, H.; Schlüter, A. D. *J. Am. Chem. Soc.* **2006**, *128*, 5091–5099.
- (26) Li, W.; Zhang, A.; Schlüter, A. D. *Macromolecules* **2008**, *41*, 43–49.
- (27) Gitsov, I.; Fréchet, J. M. J. *Macromolecules* **1993**, *26*, 6536–6546.
- (28) Helms, B.; Mynar, J. L.; Hawker, C. J.; Fréchet, J. M. J. *J. Am. Chem. Soc.* **2004**, *126*, 15020–15021.
- (29) Rajaram, S.; Choi, T.-L.; Rolandi, M.; Fréchet, J. M. J. *J. Am. Chem. Soc.* **2007**, *129*, 9619–9621.
- (30) Watanabe, N.; Mauldin, C.; Fréchet, J. M. J. *Macromolecules* **2007**, *40*, 6793–6795.
- (31) Percec, V.; Peterca, M.; Rudick, J. G.; Aqad, E.; Imam, M. R.; Heiney, P. A. *Chem.—Eur. J.* **2007**, *13*, 9572–9581.

- (32) Percec, V.; Aqad, E.; Peterca, M.; Rudick, J. G.; Lemon, L.; Ronda, J. C.; De, B. B.; Heiney, P. A.; Meijer, E. W. *J. Am. Chem. Soc.* **2006**, *128*, 16365–16372.
- (33) Percec, V.; Rudick, J. G.; Peterca, M.; Heiney, P. A. *J. Am. Chem. Soc.* **2008**, *130*, 7503–7508.
- (34) Tang, R.; Chuai, Y.; Cheng, C.; Xi, F.; Zou, D. *J. Polym. Sci., Part A: Polym. Chem.* **2005**, *43*, 3126–3140.
- (35) Cheng, C.-X.; Huang, Y.; Tang, R.-P.; Chen, E.-Q.; Xi, F. *Macromolecules* **2005**, *38*, 3044–3047.
- (36) Yi, Z.; Liu, X.; Jiao, Q.; Chen, E.; Chen, Y.; Xi, F. *J. Polym. Sci., Part A: Polym. Chem.* **2008**, *46*, 4205–4217.
- (37) Cheng, C.-X.; Jiao, T.-F.; Tang, R.-P.; Chen, E.-Q.; Liu, M.-H.; Xi, F. *Macromolecules* **2006**, *39*, 6327–6330.
- (38) Zhang, Y.; Xu, Z.; Li, X.; Chen, Y. *J. Polym. Sci., Part A: Polym. Chem.* **2007**, *45*, 3994–4001.
- (39) Zhang, Y.; Huang, J.; Chen, Y. *Macromolecules* **2005**, *38*, 5069–5077.
- (40) Percec, V.; Bera, T. K.; Glodde, M.; Fu, Q.; Balagurusamy, V. S. K.; Heiney, P. A. *Chem.—Eur. J.* **2003**, *9*, 921–935.
- (41) Liang, C. O.; Helms, B.; Hawker, C. J.; Fréchet, J. M. J. *Chem. Commun.* **2003**, 2524–2525.
- (42) Sato, T.; Jiang, D.-L.; Aida, T. *J. Am. Chem. Soc.* **1999**, *121*, 10658–10659.
- (43) Barner, J.; Mallwitz, F.; Shu, L.; Schlüter, A. D.; Rabe, J. P. *Angew. Chem., Int. Ed.* **2003**, *42*, 1932–1935.
- (44) Stiriba, S.-E.; Frey, H.; Haag, R. *Angew. Chem., Int. Ed.* **2002**, *41*, 1329–1334.
- (45) Cheng, C.; Schmidt, M.; Zhang, A.; Schlüter, A. D. *Macromolecules* **2007**, *40*, 220–227.
- (46) Li, W.; Zhang, A.; Feldman, K.; Walde, P.; Schlüter, A. D. *Macromolecules* **2008**, *41*, 3659–3667.
- (47) Li, W.; Zhang, A.; Schlüter, A. D. *Chem. Commun.* **2008**, 5523–5525.
- (48) Li, W.; Zhang, A.; Chen, Y.; Feldman, K.; Wu, H.; Schlüter, A. D. *Chem. Commun.* **2008**, 5948–5950.
- (49) Gao, M.; Kuang, G.-C.; Jia, X.-R.; Li, W.-S.; Li, Y.; Wei, Y. *Tetrahedron Lett.* **2008**, *49*, 6182–6187.
- (50) Karakaya, B.; Claussen, W.; Gessler, K.; Saenger, W.; Schlüter, A.-D. *J. Am. Chem. Soc.* **1997**, *119*, 3296–3301.
- (51) Freudenberg, R.; Claussen, W.; Schlüter, A.-D.; Wallmeier, H. *Polymer* **1994**, *35*, 4496–4501.
- (52) Khan, F. Z.; Shiotsuki, M.; Nishio, Y.; Masuda, T. *Macromolecules* **2007**, *40*, 9293–9303.
- (53) Bromberg, L. E.; Ron, E. S. *Adv. Drug Deliver. Rev.* **1998**, *31*, 197–221.
- (54) Verdonck, B.; Goethals, E. J.; Prez, F. E. D. *Macromol. Chem. Phys.* **2003**, *204*, 2090–2098.
- (55) Shibayama, M.; Tanaka, T.; Han, C. C. *J. Chem. Phys.* **1992**, *97*, 6842–6854.
- (56) Takei, Y. G.; Aoki, T.; Sanui, K.; Ogata, N.; Okano, T.; Sakurai, Y. *Bioconjugate Chem.* **1993**, *4*, 341–346.
- (57) Zhang, Y.; Furry, S.; Bergbreiter, D. E.; Cremer, P. S. *J. Am. Chem. Soc.* **2005**, *127*, 14505–14510.
- (58) Xu, J.; Ye, J.; Liu, S. *Macromolecules* **2007**, *40*, 9103–9110.
- (59) Jean, B.; Bokias, G.; Lee, L.-T.; Iliopoulos, I.; Cabane, B. *Colloid Polym. Sci.* **2002**, *280*, 908–914.
- (60) Chen, G.; Hoffman, A. S. *Nature* **1995**, *373*, 49–52.
- (61) Maiti, P. K.; Çağm, T.; Lin, S.-T.; Goddard, W. A. III. *Macromolecules* **2005**, *38*, 979–991.
- (62) Haba, Y.; Harada, A.; Takagishi, T.; Kono, K. *J. Am. Chem. Soc.* **2004**, *126*, 12760–12761.
- (63) Zhang, X.; Li, J.; Li, W.; Zhang, A. *Biomacromolecules* **2007**, *8*, 3557–3567.
- (64) Topp, M. D. C.; Dijkstra, P. J.; Talsma, H.; Feijen, J. *Macromolecules* **1997**, *30*, 8518–8520.
- (65) Motokawa, R.; Morishita, K.; Koizumi, S.; Nakahira, T.; Annaka, M. *Macromolecules* **2005**, *38*, 5748–5760.
- (66) Yan, J.; Ji, W.; Chen, E.; Li, Z.; Liang, D. *Macromolecules* **2008**, *41*, 4908–4913.
- (67) Wang, B.-B.; Zhang, X.; Jia, X.-R.; Li, Z.-C.; Ji, Y.; Yang, L.; Wei, Y. *J. Am. Chem. Soc.* **2004**, *126*, 15180–15194.
- (68) Wang, B.-B.; Li, W.-S.; Jia, X.-R.; Gao, M.; Jiang, L.; Wei, Y. *J. Polym. Sci., Part A: Polym. Chem.* **2008**, *46*, 4584–4593.